A Transient Radio Source near the Center of the Milky Way Galaxy

JUN-HUI ZHAO, D. A. ROBERTS, W. M. GOSS, D. A. FRAIL, K. Y. LO, R. SUBRAHMANYAN, M. J. KESTEVEN, R. D. EKERS, D. A. ALLEN, M. G. BURTON, J. SPYROMILIO

In late December 1990, a new radio source appeared near the center of our galaxy rivaling the intensity of Sgr A* (the compact radio source at the galactic center). Following its first detection, the flux density of the galactic center transient (GCT) increased rapidly to a maximum 1 month later, and then declined gradually with a time scale of about 3 months. Surprisingly, the GCT maintained a steep radio spectrum during both its rising and decay phases. The neutral hydrogen (HI) absorption shows similar absorption to that in front of Sgr A*; this indicates that the GCT lies near the galactic center. Furthermore, both HI and OH observations show an additional deep absorption at +20 kilometers per second with respect to the local standard of rest. Thus, the GCT is either embedded in or located behind a molecular cloud moving with that velocity. The cloud can be seen on infrared images. Its opacity is shown to be inadequate to conceal a supernova near the galactic center. It is argued that the GCT was probably transient radio emission from synchrotron-radiating plasma associated with an x-ray binary system.

DURING THE LAST TWO DECADES, A VARIETY OF INTERESTing objects has been discovered in the central region of our galaxy. These include the arcs and filaments (*1*); Sgr A East (*2*) (a probable supernova remnant); Sgr A West (*3–5*), the spiral HII region; a compact radio source (*6*), Sgr A*; a group of infrared sources (7); and the 511-keV electron-positron annihilation line (*8*). The nature of many of these objects is still not understood. One of the more intriguing is Sgr A*, the compact source believed to lie at the dynamical center of the galaxy and a low luminosity counterpart to the powerful extragalactic compact radio sources found in quasars and radio galaxies (*9*). These discoveries have established the extreme nature of the galactic center region, and considerable observational and theoretical efforts have been directed toward understanding these peculiar objects and the relationships between the various observed structures (*9*).

During a program of monitoring the radio variability of Sgr A* with the Very Large Array (VLA) of the National Radio Astronomy Observatory (NRAO) (*10*), a transient radio source, hereafter called the galactic center transient (GCT), was first detected in images observed on 28 December 1990 at wavelengths 1.3, 2, and 3.6 cm (*11*). It had not appeared in images of 11 December 1990 at the same frequencies, nor had anything been seen during the monitoring VLA program of observations every 2 weeks since 1 March 1990. Shortly after the discovery, the Australia Telescope (AT) of the Australia Telescope National Facility (ATNF) detected the GCT at 6 and 20 cm and found the continuum emission at 20 cm to be at least as strong as Sgr A*. The GCT is located 35.5″ southeast of Sgr A* and adds a new puzzle to the galactic center region. The GCT is not related to a previous radio transient event (*12*) which is 80″ away from the new transient source and was observed with the Jodrell Bank radio-linked interferometers in 1975 and identified with the transient x-ray source A1742-28.

Following the radio detection of the GCT, radio and infrared observations were conducted using the VLA, the Very Long Baseline Array (VLBA), the AT, and the Anglo Australian Telescope (AAT) to determine the location of GCT with respect to the various other structures in the central region of the galaxy, to measure its angular size, and to monitor the temporal variations in the spectral energy distribution.

Observations and data reduction. The measurements of the flux density of the GCT at the wavelengths from 1.3 to 22 cm were made with the VLA and the AT on 30 epochs from 11 December 1990 to 17 August 1991. The VLA observations used the radio source 3C 286 as the primary flux density calibrator (*13*). The radio sources 1748–253 and NRAO 530 were used to calibrate the complex gains and 3C 286 also served to calibrate the band pass in spectral-line observations. For each observation, data reduction was performed using the Astronomical Image Processing System (AIPS) of NRAO (*14*). Figure 1 shows VLA images at 3.6 cm of the Sgr A West region that were made before and after the GCT appeared.

The observations of the GCT with the AT used the 6-km array configuration. The visibility data were calibrated in amplitude and phase by means of periodic observations of the unresolved calibrator, 1748–253. The flux density scale was established with a short observation of the primary calibrator 1934–638. The spectral visibilities obtained on 1934–638 were also used to calibrate the band pass in the case of spectral-line observations. Images were constructed using only the calibrated visibilities at higher spatial frequencies (where the diffuse emission from the galactic center region was well resolved) in order to reduce the errors due to confusion. Nevertheless, the dynamic range in the final deconvolved images, and hence the uncertainties in the derived flux densities of the GCT at various epochs, is limited by confusion from nearby extended emission rather than thermal noise. Owing to the complexity of the region and the limited number of instantaneous visibility measurements at the AT, no self-calibration techniques were applied.

Jun-Hui Zhao, D. A. Roberts, W. M. Goss, and D. A. Frail are at the National Radio Astronomy Observatory, P.O. Box 0, Socorro, NM 87801. K. Y. Lo is in the Astronomy Department, University of Illinois, 1002 West Green Street, Urbana, Illinois 61801. R. Subrahmanyan, M. J. Kesteven, and R. D. Ekers are at the Australia Telescope National Facility, P.O. Box 76, Epping, New South Wales 2121, Australia. D. A. Allen, M. G. Burton, and J. Spyromilio are at the Anglo Australian Observatory, P.O. Box 296, Epping, New South Wales 2121, Australia.

Very Long Baseline Interferometry (VLBI) observations at 3.6 cm were made on 18 March with the phased VLA and the four available antennas of the VLBA (Pie Town, Los Alamos, North Liberty, and Owens Valley). The maximum baseline between the VLA and Pie Town is about 50 km. During the total observing time of 1.5 hours we alternated between 5-minute scans on NRAO 530 and 20-minute scans on the GCT. The data acquired on NRAO 530 were used to re-phase the VLA during the observations and to act as a "fringe finder" during correlation and data reduction. The data were recorded on MkII tapes with a bandwidth of 2 MHz and these tapes were processed on the NRAO MkII correlator. After correlation, the data were reduced with AIPS following standard procedures. The relative visibility amplitude was measured for each baseline after delay and fringe fitting. No attempt was made to image these data.

Temporal variations in the radio continuum emission of the GCT. Radio light curves at wavelengths from 1.3 to 22 cm, observed from 11 December 1990 to 17 August 1991, are shown in Fig. 2. The GCT was not present at wavelengths 1.3, 2, and 3.6 cm on the first date: upper limits to the flux density are 8, 5, and 4 mJy, respectively. The GCT was first detected on 28 December 1990 in VLA images at all three wavelengths. About 3 weeks later, around 20 January 1991 (±1 week), the radio continuum emission reached a peak. Thereafter, the flux density decayed slowly following a power law. At 6 cm, measurements were made at only a few epochs, and the flux density appeared to decrease at a similar rate. The evolution of the flux density in the decaying phase can be described by $S_\nu \propto (t - t_0)^{-0.67\pm0.08}$ at wavelengths between 1.3 and 6 cm, where the best fit reference time t_0 is about late December 1990.

Variations in the flux density as large as 50 percent were observed on time scales of a week. At a wavelength of 3.6 cm, an 8-hour observation made with the VLA in February 1991 showed flux density variations less than 10 percent on time scales of 2 hours. From 17 March to 26 April 1991, five observations were made with the AT at wavelengths between 18 and 21 cm (see Fig. 2). On 17 March the flux density of the continuum emission at 21 cm exceeded that of Sgr A*. Subsequently, the GCT declined at a rate of about 22 mJy per day, reaching a minimum on 17 April. Throughout this period there were no significant variations in the flux density of Sgr A*. The last AT observation, on 26 April, indicated a rejuvenation of the GCT. The VLA began observations at these wavelengths in early June and confirmed that the flux density was indeed rising for the second time. It attained a secondary maximum of 540 mJy at 20 cm on 17 July 1991.

Comparison of OH and HI absorption spectra between the GCT and Sgr A* and the location of the GCT. OH absorption spectra toward the GCT and Sgr A* were obtained with the AT on 4 April. The Λ-doubling transitions of the hydroxyl radical OH at 1665 and 1667 MHz were simultaneously observed with a velocity resolution of 2.8 km s^{-1}. The results are shown in Fig. 3. Panel A shows a contour representation of the image of the galactic center region in the continuum emission adjacent to the OH lines. The absorption spectra obtained toward the GCT and Sgr A* are shown in panels B and C, respectively. In contrast to Sgr A*, the spectrum toward the GCT shows strong absorption at an LSR velocity of +20 km s^{-1}. Clearly, there is dense molecular gas along the line of sight to the GCT. Images of the galactic center region in ammonia emission (*15*) have indeed shown the presence of a molecular gas clump at the position of the GCT, with a velocity of +20 km s^{-1}.

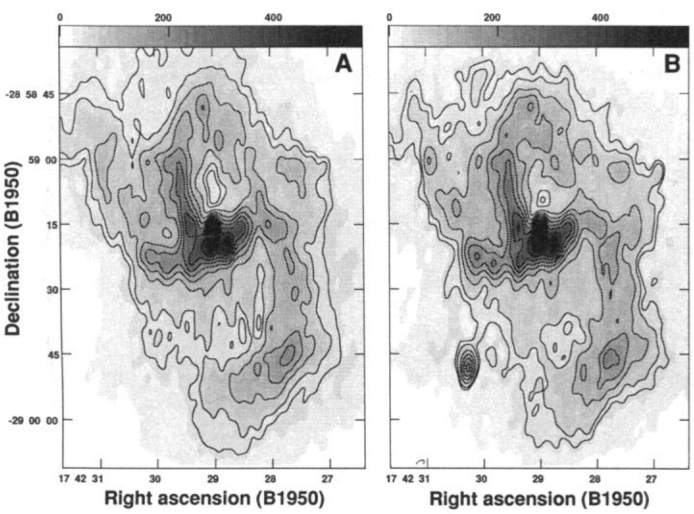

Fig. 1. The VLA snapshot images of Sgr A West at 3.6 cm, (**A**) before the GCT on 11 December 1990 and (**B**) during the GCT on 20 January 1991. The contours are −3, 3, 4, 7, 11, 16, 22, 29, 37, 46, 56, 67, 79, 92 × 10^{-2} Jy per beam. The gray scale flux density range is 0 to 0.55 Jy per beam. The beam sizes (FWHM) are 4.9″ × 2.1″ (PA = −3.9°) and 4.9″ × 2.2″ (PA = −4.9°) for the images (A) and (B), respectively. At all wavelengths the measured position indicates an angular separation of the GCT from Sgr A* of 35.5″. Adopting a position RA(B1950) = 17^h 42^m 29.^{s}318, Dec(B1950) = −28°59′18.39″ for Sgr A* (*41*), the GCT is located at RA(B1950) = 17^h 42^m 30.^{s}598 (±0.^{s}010), Dec(B1950) = −28°59′49.69″ (±0.10″).

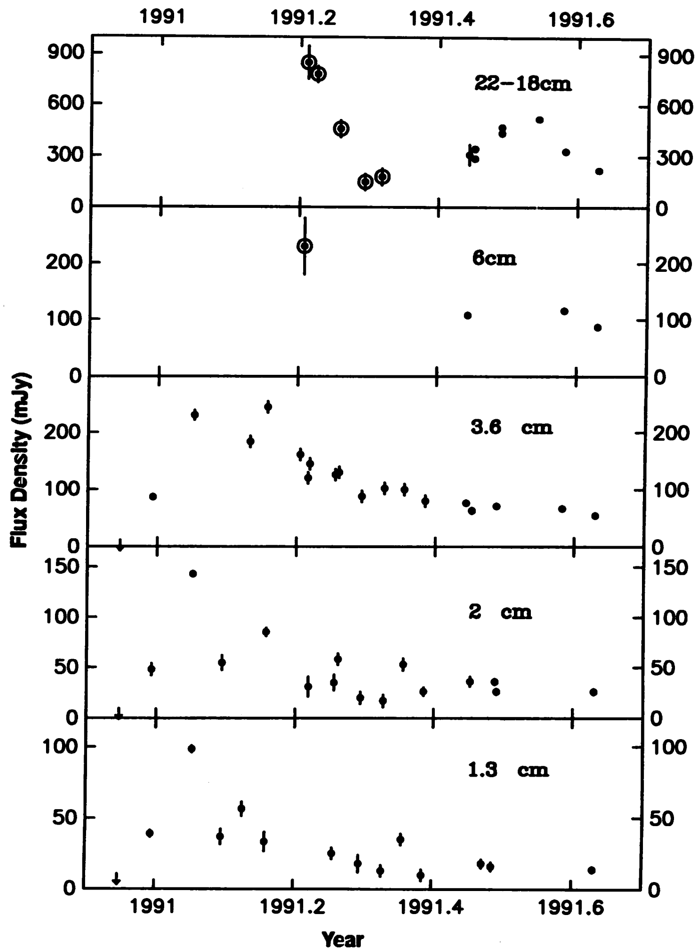

Fig. 2. Radio flux density of the GCT as a function of time at 1.3, 2, 3.6, 6, and 18 to 22 cm. The VLA measurements are indicated by dots. During our observations, the VLA was reconfigurated from C (early November 1990 to late January 1991), CnD (early and middle February 1991), D (late February 1991 to late May 1991) to A array (early June 1991 to late September 1991). The circled dots denote the AT measurements. Uncertainties attributable to random errors are indicated by vertical bars whenever they exceed the symbol sizes.

No significant ammonia emission has been detected toward Sgr A* (*15*). Our observations locate the GCT behind or perhaps even embedded within this molecular gas clump.

To estimate the distance of the GCT, we observed neutral hydrogen (HI) absorption using the AT and the VLA. The same features are seen with both instruments. Figure 4 shows HI absorption spectra toward the GCT and Sgr A* made with the VLA on 17 July 1991. Panel A is a contour representation of the continuum emission at 21 cm; panels B and C show the HI absorption spectra toward the GCT and Sgr A*, respectively. Several velocity components are present in the spectra of both objects. The saturated absorption at $\nu = 0$ km s^{-1} in the two spectra is that expected from the integrated path length to the galactic center. Three components with peculiar velocities are also seen in both sources. The feature at $\nu = -54$ km s^{-1} is attributed to the expanding "3-kpc arm." The component at $\nu = -135$ km s^{-1} arises from the front of the "expanding molecular ring" (*16, 17*). The absorption at $\nu = +60$ km s^{-1} is attributed to the circumnuclear disk (*18*). At a velocity of +20 km s^{-1}, the HI absorption spectrum shows increased HI column density toward the GCT, just as is the case for OH but the +20 km s^{-1} feature is blended with features at 0 and +60 km s^{-1}. The similarity of these absorption features in the two sources indicates that the GCT lies at or beyond the distance to Sgr A*.

Measurement of the angular size. On 18 March 1991, an MkII VLBI observation was carried out. Fringes were detected on only the shortest baseline, VLA to Pie Town. In June several high-resolution observations were made at 1.3, 2, 3.6, 6, and 20 cm with the VLA in the largest (A) configuration. These confirmed that the source was resolved. Figure 5 shows the high-resolution VLA images of the GCT made on 26 June and 28 June 1991 at 1.3 and 2 cm, respectively. The intrinsic shape of the source has been estimated by fitting two-dimensional Gaussian models to the image after deconvolution with the telescope beams. The model fits indicate sizes of ~0.16″ × 0.04″ at a position angle (PA) of 28°. The measurements of the intrinsic shape in the two independent observations and at different wavelengths agree within the errors.

The high-resolution VLA measurements of the angular size were

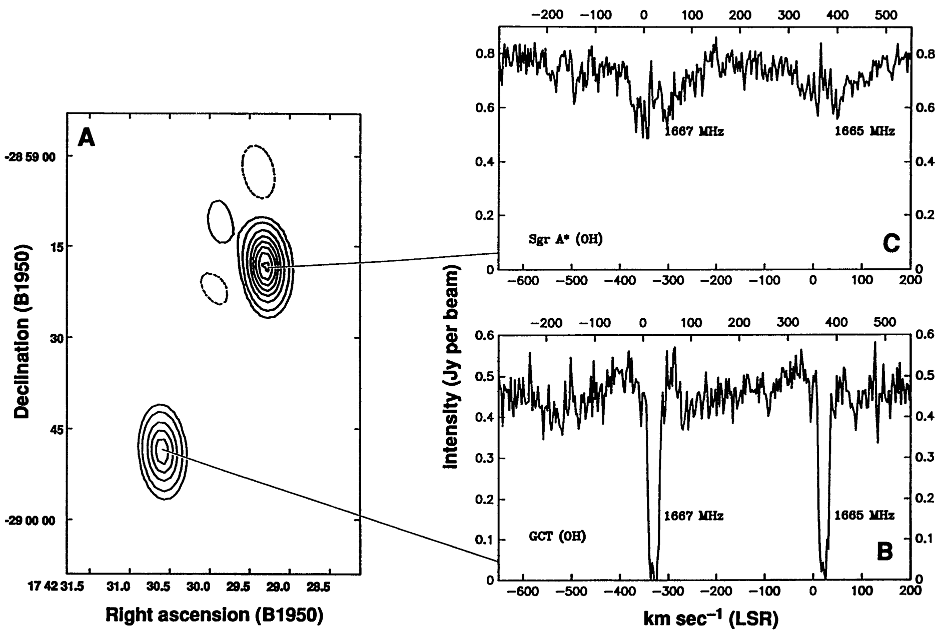

Fig. 3. Absorption spectra of the 1665- and 1667-MHz transitions of the OH radical obtained towards the GCT and Sgr A* with the AT on 4 April 1991 with a velocity resolution 2.8 km s^{-1}. Panel (**A**) shows an image of the continuum emission and panels (**B**) and (**C**) show the spectra toward the GCT and Sgr A*, respectively. The beam has a size (FWHM) 8.6″ × 4.1″ at a position angle of 4° and the contours are at −5, 5, 10, 15, 20, 30, 40, 50, 60, 70 × 10^{-2} Jy per beam. The velocity scale on the bottom (or the top) has its origin at the LSR velocity corresponding to the rest frequency of the 1665 MHz (or 1667 MHz) OH transition.

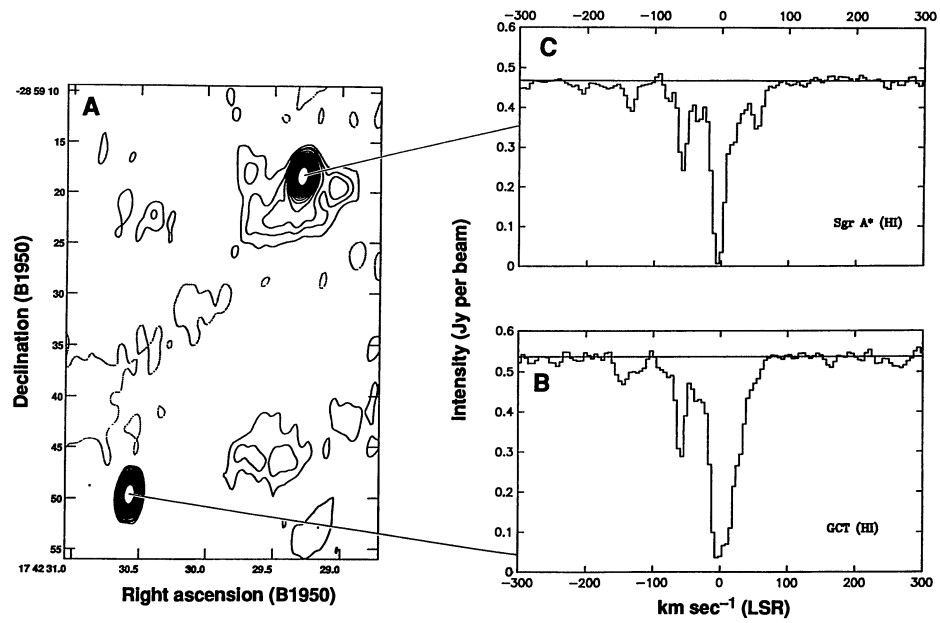

Fig. 4. Comparison of HI absorption spectra between (**B**) the GCT and (**C**) Sgr A*. Panel (**A**) is the image of the continuum emission at 21 cm with contours plotted at −5.4, 5.4, 9.0, 12.6, 19.8, 28.8, 39.6, 52.2, 66.6, 82.8, 101, 121, 142, 166, 191, 218, 247, 277 mJy per beam (FWHM = 2.2″ × 1.0″). The observations were made on 17 July 1991 with the VLA. The spectral resolution is 6.2 km s^{-1}.

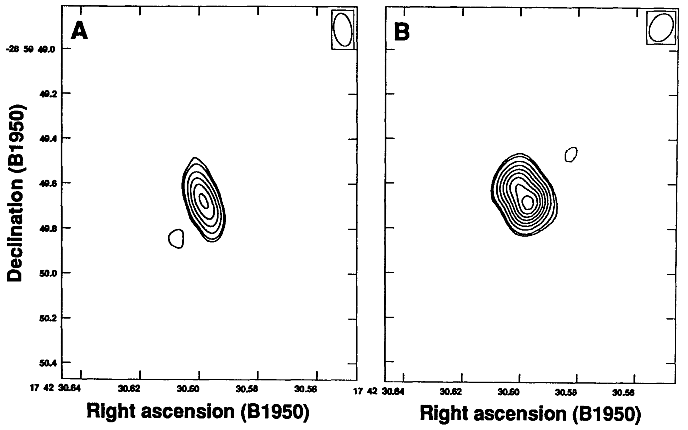

Fig. 5. High-resolution images of the GCT observed with the VLA (**A**) on 26 June 1991 at 1.3 cm; with contours at −1.8, 1.8, 2.4, 4.2, 6.6, 10.8, 13.2 mJy per beam; (**B**) on 28 June 1991 at 2 cm, with contours at −1.5, 1.5, 2.0, 3.5, 5.5, 8.0, 11.0, 14.5, 18.5, 23.0 mJy per beam. The beams are indicated in the upper right corners of the images and have dimensions (FWHM) 0.15″ × 0.079″ (P.A. = 8.9°) and 0.13″ × 0.10″ (P.A. = −30°) at 1.3 and 2 cm, respectively. Both images show the source to be extended roughly along the galactic plane.

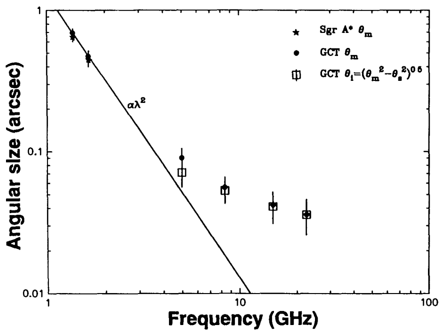

Fig. 6. The angular size of the GCT as a function of observing frequency. The measurements between 1.37 and 8.4 GHz were made in the (u-v) visibility domain by Gaussian fitting the long-baseline visibility data. The observed angular size of the GCT at 20 cm (1.37 and 1.65 GHz) agrees approximately with that of Sgr A* and has a λ^2 dependence on observing wavelength. The square symbols represent the intrinsic size derived by deconvolution assuming a disk scattering model.

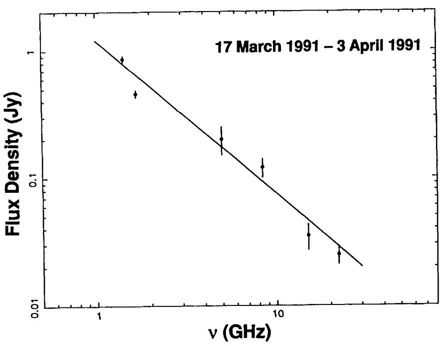

Fig. 7. Radio spectrum of the GCT, observed from 17 March to 3 April 1991 at times near the recorded maximum value at 20 cm (the dots), fitted with a power law spectrum with a spectral index −1.2 (the solid line).

made at six frequencies (1.37 to 22.5 GHz, see Fig. 6) during June 1991 when the VLA was in the A configuration. The dots in Fig. 6 represent the measured angular size (θ_m) of the GCT. At wavelengths between 22 and 18 cm, the angular size is nearly the same as Sgr A* and shows the same λ^2 dependence of angular size on observing frequency as Sgr A*. In Sgr A*, this λ^2 dependence has been observed from 1 to 22.5 GHz (*19*) and is attributed to interstellar scattering (*9, 20*). The straight solid line labeled $\propto \lambda^2$ represents this functional dependence. We note that the radio transient source in 1975 also had the same angular size at 0.96 GHz as Sgr A* (*12*). Interstellar scattering is thus the dominant cause of angular broadening in the GCT at wavelengths longer than 6 cm.

If the GCT were located beyond the galactic center, the increased interstellar material along the line of sight should scatter-broaden the GCT to be significantly larger than Sgr A*. Again we infer that the GCT must be nearly at the same distance as Sgr A*. We therefore adopt a distance of 8.5 kpc to the GCT.

The measured angular size at wavelengths shorter than 6 cm appears substantially larger than the expected scattering size (θ_s) and suggests that the source is resolved. The intrinsic angular size (θ_i) can be estimated by quadratic deconvolution of θ_s from the measured diameter, according to a disk scattering model. The results are also plotted in Fig. 6, which shows that at wavelengths below about 4 cm the observed size is a good estimate of the intrinsic size and is not affected by scatter broadening. The corresponding linear dimensions are 18×10^{15} and 4×10^{15} cm (about 7 × 2 light-days). The major axis is approximately aligned with the galactic plane and the structure is indicative of a source expanding with an average rate of about 6000 km s^{-1} in the galactic plane (assuming that the expansion started as a point source in December 1990).

The nature of the radio radiation from the GCT. If the GCT radiates isotropically, we compute a total radio luminosity of 1×10^{33} erg s^{-1} over the frequency range 1 to 25 GHz. The radio spectrum close to the epoch of maximum flux density at 20 cm is shown in Fig. 7. At wavelengths between 1.3 and 20 cm, the spectrum is described by a power law ($S_\nu \propto \nu^\alpha$) with a spectral index $\alpha = -1.2$. The spectral index at wavelengths below 6 cm was about −1 at all epochs. The distinctive flux density variations at 20 cm imply a flattening of the spectrum above 11 cm during April and May. The measurements of the angular size and flux density at 22 cm indicate that the source has a brightness temperature exceeding 7×10^5 K. The steep radio spectrum and the high brightness temperature indicate that the emission is nonthermal and probably synchrotron radiation.

A number of VLA observations were made at 3.6 and 2 cm in March, June, and July to measure the polarization properties of the GCT. No polarized flux density was detected, and the fractional linear polarization was found to be less than 2%. This may not be surprising. There have been no detections of polarized emission from other nonthermal radio sources in Sgr A. From estimates of the emission measure (*4*) (4×10^6 cm^{-6} pc) and electron density (4×10^3 cm^{-3}), along with an estimate of the magnetic field strength along the line of sight (*21*) (1 mG), we infer the Faraday rotation measure to be 8×10^5 rad m^{-2}. The large Faraday rotation measure probably arises mainly from the circumnuclear disk region. At 2 cm this large rotation measure would result in a rotation of the polarization position angle by about 120° across the VLA observing band of 50 MHz. Therefore, the nondetection of polarization in the radio emission from the GCT, as well as from other nonthermal sources in the galactic center region, is likely the result of severe depolarization.

Infrared images of the region. Infrared images of the galactic center have been taken on several occasions with the new infrared camera IRIS (*22*) on the 3.9-m Anglo-Australian Telescope. A set of images at H (1.65 μm) and K′ (2.11 μm) bands with 0.78″ pixel scale was obtained on 6 May 1991. These images are dominated by stellar emission from the galactic nucleus. The density of stars in this field is relatively high and the infrared images are limited by confusion with stellar emission. However, several dark regions or clouds are notable, in which the stellar density is considerably lower. These clouds lie along the circumnuclear disk which surrounds Sgr A West and is observed in HCN and HCO+ ($J = 1 - 0$) line emission (*18, 23*). More clouds are observed to the southeast of the images, parallel to the galactic plane. The position of transient source was located by reference to the M supergiant IRS 7, whose

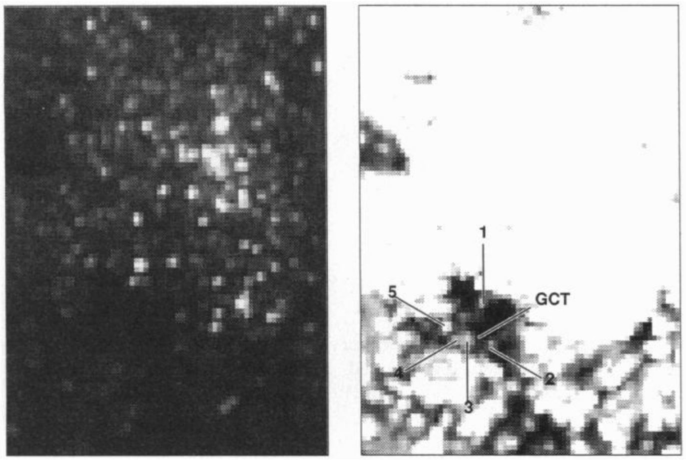

Fig. 8. Portion of an image at K′ of the galactic center region reproduced at two gray scales. (**Left**) Showing IRS 7 (the brightest source) and the IRS 16 complex below it. (**Right**) The same area at a grey scale range such that the diffuse starlight saturates and only molecular clouds appear dark. The position of the GCT is marked. The five brightest infrared sources surrounding were measured. North is top, east to left.

position (*24*) is known with respect to Sgr A*. The GCT is found to lie within the largest obscuring cloud along the southeast rim of the circumnuclear disk. Also, a concentration of ammonia emission gas (*15*) at +20 km s^{-1} is coincident with this dark cloud. Figure 8 shows a portion of the K′ image in which the galactic nucleus and the clouds in the circumnuclear disk are observed. The location of the GCT is indicated. This image is displayed at two different gray scale levels to show both stellar continuum and the (faint) stars visible within the obscuring clouds.

There are several sources within the cloud. These are mostly pointlike, and we will assume that the brightest five sources are therefore stars (see Fig. 8). However, we note that some sources (for example, star 3) are slightly extended and may represent gaps in the cloud. We have attempted to extract photometry of the five brightest sources. The greatest uncertainty in doing so lies in choosing the appropriate sky level, because outside this and other molecular clouds the image is confusion-limited. We chose a region within the cloud devoid of obvious sources to define the sky level. The nearby bright sources IRS 9 and IRS 19 provided the photometric zero point, interpolating existing H and K photometry (*25, 26*) for the IRIS filters. In Table 1 we list the derived K′ magnitudes and H-K′ colors. The H-K′ colors of most sources in the galactic center region are close to 2.0 mag, of which about 0.2 mag is intrinsic and the remainder due to reddening of A_V to about 30 mag. Sources 2 and 5 appear to have similar colors, and thus probably lie in front of the cloud, while the other three are redder by up to 1 mag in H-K′. The probability is high that these are background sources seen through the cloud, and on this assumption we infer that the additional extinction through the cloud is about 1 mag at K′, or about 15 mag of A_V. If, instead, the source lies within the cloud this is a lower limit to the extinction.

Table 1. K′ magnitudes and H-K′ colors of IR sources near the GCT.

Source	K′	H-K′
1	13.3 ± 0.4	3.0 ± 0.6
2	13.4 ± 0.4	1.7 ± 0.4
3	12.7 ± 0.2	2.7 ± 0.3
4	12.9 ± 0.3	2.8 ± 0.4
5	12.7 ± 0.2	1.5 ± 0.2

An alternative estimate of the cloud opacity is to compare the integrated intensity in the cloud with that in regions at the same radial distance from the galactic center. Again some uncertainty is introduced by the unknown sky level of the image. We set the sky level according to the darkest portion of the image, in particularly dense molecular clouds about five times more distant from the galactic center. We took mean intensities at five positions all equally separated from Sgr A* and derived the extinction through the molecular cloud on the assumption that the radiation seen therein is the same but for attenuation. On this basis we derive an extinction $A_{K'} = 2.5 \pm 0.4$ mag. This too is potentially an underestimate because some unresolved foreground stars will be seen superimposed on the cloud.

In addition, a column density of molecular hydrogen in this cloud [$N(H_2) \approx 4 \times 10^{22}$ cm^{-2}] derived from NH_3 spectra (*27*) provides an estimate of $A_{K'} \sim 2$, while the $N(H_2)$ (2×10^{23} cm^{-2}) derived (*28*) from our OH absorption spectra of the +20 km s^{-1} feature is somewhat higher. Nevertheless, the extinction estimated via molecular spectra agrees roughly with the infrared estimates.

Conservatively we take the total extinction to the GCT to be double that of a typical clump plus the interstellar component, or $A_{K'} \sim 6$ mag. We can place a limit on the apparent K′ magnitude of the GCT of $m_{K'} > 13$, which corresponds to 7 after correction for this reddening. The corresponding absolute magnitude limit is $M_{K'} > -7.5$. In other words, the GCT was not brighter than −7.5 in absolute K′ magnitude in May.

Examination of an earlier image, taken in March under poorer seeing, shows no additional source above about the same magnitude limit. We have also examined an image taken by C. Aspin (*29*) before the GCT erupted and again find no indication that the GCT had any infrared counterpart.

Discussion and conclusions. The radio properties of the GCT are summarized in Table 2. Here we compare them to other transient events in an attempt to determine the nature of the object.

The radio spectrum of the GCT cannot be interpreted as thermal bremsstrahlung from a standard nova shell (*30*). The peak luminosity was about 200 times larger than the 1985 radio outburst of RS Oph, a recurrent nova (*31*). The observations are also inconsistent with that outburst, in which the radio emission comprised a thermal short-wavelength component and a non-thermal long-wavelength component (*32*). We thus rule out nova-like events.

The peak luminosity of the GCT was close to that of the prompt radio outburst from supernova (SN) 1987A (*33*). But typical type II SNs have radio luminosities a factor 10^3 larger. The extremely elongated morphology of the GCT and low inferred expansion rate (6000 km s^{-1}) argue against an interpretation as an SN. No significant emission was found at the location of the ^{56}Co lines (847 and 1238 keV) in a γ-ray spectrum (200 keV to 1.5 MeV) observed in July 1991 toward the galactic center with the OSSE spectrometer

Table 2. Radio properties of the GCT.

Radio luminosity:	1×10^{33} (erg s^{-1})		
Radio spectrum:	$\alpha \sim -1.2$ ($S_\nu \propto \nu^\alpha$)		
Shape and linear size:	18×4 (10^{15} cm)		
Linear polarization*:	<2%		
Radio light curve:	1. a month to reach maximum		
	2. decline following $\nu^{-1.2}(t - t_0)^{-0.67}$		
Fluctuation of flux density:	λ(cm)	ΔS/2S(%)	Time scale
	20	65	4 weeks
	6	. . .	. . .
	3.6	35	2 weeks
	2	50	1 week
	1.3	55	1 week

*Measured at 2 and 3.6 cm with a bandwidth 50 MHz.

of the GRO (*34*). The ^{56}Co are high-energy signatures for an SN and were detected from SN 1987A (*35*). The limit on the absolute K′ magnitude also effectively discounts the possibility that the GCT is a supernova of any recognized type. Even the underluminous SN 1987A lay well above the derived limit for the first 2.5 years.

The peak radio luminosity of the GCT is comparable to that of the radio outbursts from x-ray binary systems, such as Circinus X-1 (*36*) and V404 Cyg (*37*). But the flux-density variations in the GCT are unlike those of x-ray binaries such as Cygnus X-3, in which the radio emission is characterized by a multiplicity of apparently discrete bursts and by abrupt flux-density changes (*38*). However, it is possible that the transient radio emission of the GCT is attributable to an ejection of relativistic plasma from an x-ray transient source such as V404 Cyg (*37*). The radio emission from the GCT has similar characteristics to V404 Cyg, namely a steep spectrum, power-law decay, and 10^{33} erg s^{-1} peak luminosity. The elongated morphology and linear size of the GCT are similar to the observed radio structures in x-ray binary systems like Cyg X-3 (*39*).

Transient x-ray sources are thought to be binary systems in which a neutron star or black hole accretes material from its companion (*40*). Radio bursts from x-ray transients are often strongly correlated with their x-ray bursts. The HI column density toward the galactic center (about 10^{23} cm^{-2}) should not significantly attenuate radiation with energy above about 1 keV. The detection of a transient x-ray source at the position of the GCT would be important evidence in support of this hypothesis.

REFERENCES AND NOTES

1. F. Yusef-Zadeh, M. Morris, D. Chance, *Nature* **301**, 557 (1984).
2. R. D. Ekers, W. M. Goss, V. J. Schwarz, D. Downes, D. Rogstad, *Astron. Astrophys.* **43**, 159 (1975).
3. R. L. Brown, K. J. Johnston, K. Y. Lo, *Astrophys. J.* **250**, 155 (1981).
4. R. D. Ekers, J. H. van Gorkom, V. J. Schwarz, W. M. Goss, *Astron. Astrophys.* **122**, 143 (1983).
5. K. Y. Lo and M. J. Claussen, *Nature* **306**, 647 (1983).
6. B. Balick and R. L. Brown, *Astrophys. J.* **194**, 265 (1974).
7. E. E. Becklin and G. Neugebauer, *Astrophys. J. Lett.* **200**, L71 (1975).
8. See, for example, a review by R. E. Lingenfelter and R. Ramaty, in *The Center of The Galaxy*, M. Morris, Ed. (IAU Symp. 136, Kluwer Academic, Dordrecht, 1989), pp. 587–605. Recent results about the position and spectrum of 511-keV source were discussed by G. K. Skinner *et al.* [*Astron. Astrophys.* **252**, 172 (1991)], R. Sunyvea *et al.* [*Astrophys. J. Lett.* **383**, L49 (1991), and L. Bouhet *et al.*, *ibid.*, p. L45].
9. K. Y. Lo, in *The Center of The Galaxy*, M. Morris, Ed. (IAU Symp. 136, Kluwer Academic, Dordrecht, 1989), pp. 527–534.
10. Jun-Hui Zhao, W. M. Goss, K. Y. Lo, R. D. Ekers, in *Relationships between Active Galactic Nuclei and Starburst Galaxies*, A. Filippenko, Ed. (Astronomical Society of the Pacific, San Francisco, in press).
11. Jun-Hui Zhao, D. A. Roberts, W. M. Goss, D. A. Frail, K. Y. Lo, R. D. Ekers, *Int. Astron. Union Circular No. 5210* (1991).
12. R. D. Davies, D. Walsh, I. W. A. Browne, M. R. Edwards, R. G. Noble, *Nature* **261**, 476 (1976).
13. The flux density of 3C 286 was given by Rick Perley (1990 VLA Calibrator Manual, NRAO, Socorro).
14. For each VLA observation, an iterative procedure of deconvolution [T. Cornwell and R. Braun, in *Synthesis Imaging in Radio Astronomy*, R. A. Perley, F. R. Schwab, A. H. Bridle, Eds. (Astronomical Society of the Pacific, San Francisco, 1989) pp. 167–184] and self-calibration [T. Cornwell and E. B. Fomalont, in *ibid.*, pp. 185–196] was performed. The flux density of the GCT was derived in each observation from the final deconvolved image that was made after subtracting the confusing emission from the HII region Sgr A West. The root-mean-square noise in the VLA images ranged from 0.5 to 10 mJy depending on the observing time.
15. P. T. P. Ho *et al.*, *Nature* **350**, 309 (1991).
16. H. S. Liszt and W. B. Burton, *Astrophys. J.* **236**, 779 (1980).
17. ______, J. M. van der Hulst, *Astron. Astrophys.* **142**, 245 (1985).
18. R. Genzel, in *The Center of The Galaxy*, M. Morris, Ed. (IAU Symp. 136, Kluwer Academic, Dordrecht, 1989), pp. 393–405.
19. K. Y. Lo, in *The Galactic Center*, D. C. Backer, Ed. (American Institute of Physics, New York, 1987), pp. 30–38.
20. R. D. Davies, D. Walsh, R. S. Booth, *Mon. Not. R. Astron. Soc.* **177**, 319 (1976).
21. N. E. B. Killeen, K. Y. Lo, R. Crutcher, *Astrophys. J.*, in press.
22. D. A. Allen, *Proc. Astron. Soc. Aust.* **9**, in press.
23. M. C. H. Wright, J. M. Marr, D. C. Backer, in *The Center of The Galaxy*, M. Morris, Ed. (IAU Symp. 136, Kluwer Academic, Dordrecht, 1989), pp. 407–410.
24. F. Yusef-Zadef and M. Morris, *Astrophys. J. Lett.* **371**, L59 (1991).
25. E. E. Becklin, K. Matthews, G. Neugebauer, S. P. Willner, *Astrophys. J.* **219**, 121 (1978).
26. D. A. Allen, A. R. Hyland, D. J. Hillier, *Mon. Not. R. Astron. Soc.* **244**, 706 (1990).
27. A concentration of NH_3 emission in the $(J,K) = (3,3)$ line has been found by Ho *et al.* (*15*) at the position of the GCT. The authors have also shown that the clump is a part of an elongated molecular streamer which connects the galactic center to the giant molecular cloud (M-0.13-0.08). Indeed, this clump is not observed in the images of NH_3 (1,1) and (2,2) lines from the Nobeyama Millimeter Array owing to the fact that the beam-averaged excitation temperature is probably lower than the brightness temperature of the continuum emission from Sgr A West [S. K. Okumura *et al.*, *Astrophys. J.* **378**, 127 (1991)]. However, the H_2 column density of the molecular cloud at the position of the GCT should be similar to the mean H_2 column density (4×10^{22} cm^{-2}) of the streamer (or "finger") derived by Okumura *et al.*
28. The OH column density of the molecular cloud can be estimated from the OH absorption spectra using a formula [B. E. Turner, *Astrophys. J.* **186**, 357 (1973)]:

$$\left[\frac{N(\mathrm{OH})}{\mathrm{cm}^{-2}}\right] = 4.24 \times 10^{14}\tau\left[\frac{T_s}{10\mathrm{K}}\right]\left[\frac{\delta v}{1\mathrm{kHz}}\right] \quad (1)$$

where τ refers to the optical depth at the center of the 1667 line and $\delta\nu$ is the full line width at half intensity. For the +20 km s^{-1} feature, given $\tau \approx 3$ and $\delta\nu \approx 110$ kHz (20 km s^{-1}), under the assumption of the excitation temperature T_s = 10K, N(OH) is estimated to be 1.4×10^{17} cm^{-2}. Assuming that the fractional abundance of OH to H_2 is 6×10^{-7} [see E. Herbst and C. M. Leung, *Astrophys. J. Suppl.* **69**, 271 (1989)], the H_2 column density of the +20 km s^{-1} molecular is about 2×10^{23} cm^{-2}.
29. C. Aspin, private communication.
30. See, for example, a review by E. R. Seaquist, in *Classical Novae*, M. F. Bode and A. Evans, Eds. (Wiley, New York, 1989), pp. 143–161.
31. R. M. Hjellming *et al.*, *Astrophys. J. Lett.* **305**, L71 (1987).
32. A. R. Taylor, R. J. Davis, R. W. Porcas, M. F. Bode, *Mon. Not. R. Astron. Soc.* **237**, 81 (1989).
33. A. J. Turtle *et al.*, *Nature* **327**, 7 (1987).
34. B. Purcell, private communication.
35. The γ-ray lines from SN 1987A were first detected by S. M. Matz *et al.*, *Nature* **331**, 416 (1988).
36. J. A. J. Whelan *et al.*, *Mon. Not. R. Astron. Soc.* **181**, 257 (1977).
37. X. Han and R. M. Hjellming, in *Accretion-Powered Compact Binaries*, C. W. Mauche, Ed. (Cambridge Univ. Press, New York, 1990), pp. 25–28.
38. R. M. Hjellming, R. L. Brown, L. C. Blankenship, *Astrophys. J. Lett.* **194**, L13 (1974).
39. L. A. Molnar, M. J. Reid, J. E. Grindlay, *Astrophys. J.* **331**, 494 (1988).
40. J. van Paradijs and F. Verbunt, in *High Energy Transients in Astrophysics*, S. E. Woosley, Ed. (American Institute of Physics, New York, 1984), pp. 49–58.
41. D. Backer, private communication.

42. We thank R. Hjellming, R. Sramek, L. Ball, K. Weiler, and B. Turner for useful discussions and comments. We also thank P. Meikle during whose time the infrared observations were made. J.H.Z. thanks the ATNF for their hospitality. The National Radio Astronomy Observatory is operated by Associated Universities, Inc., under a cooperative agreement with the National Science Foundation. The Australia Telescope National Facility is operated in association with the Division of Radiophysics by CSIRO.

9 December 1991; accepted 6 February 1992